

# Parametric optimization of cyanobacterial coagulation at exponential and decline phases by combining polyaluminum chloride and cationic polyacrylamide

Weijun Song, Yu Xie, Jiapeng Hu, Xunfang Wu and Xi Li 

## ABSTRACT

*Microcystis* spp. is the most common and problematic species during cyanobacterial bloom. This study employed *Microcystis aeruginosa* for coagulation experiments. Effects of polyaluminum chloride (PAC), cationic polyacrylamide (CPAM), and pH value on cyanobacterial removal at exponential and decline phases by coagulation were investigated by measuring chlorophyll *a*. A mathematical model between factors and response variables was established using response surface methodology (RSM). Results showed that factors of CPAM dosage, PAC dosage, and pH value could strongly affect the removal ratio of *Microcystis* at both exponential and decline phases. RSM revealed that the order of influence factors on the removal of chlorophyll *a* was CPAM > PAC > pH for *Microcystis* at the exponential phase, and these orders of CPAM > PAC > pH (PAC coagulation) and CPAM > PAC > pH (CPAM coagulation) were for *Microcystis* at the decline phase. It suggested that the growth phase of cyanobacteria was also quite important to optimize the coagulation process. Besides, a fitted model was developed, and it could well predict the removal ratio of chlorophyll *a* by coagulation with various treatments. The model recommended dosages of CPAM (3.72 mg/L) and PAC (10.23 mg/L) for *Microcystis* at the exponential phase with a pH value of 8.25, and dosages of CPAM (5.98 mg/L) and PAC (17.81 mg/L) were for *Microcystis* at the decline phase with a pH value of 8.21. Overall, these results would provide a technical guideline of combining PAC and CPAM to treat cyanobacteria at exponential and decline phases.

**Key words** | cationic polyacrylamide, coagulation, cyanobacterial growth phase, polyaluminum chloride, response surface methodology, successive bloom

## HIGHLIGHTS

- Effects of PAC, CPAM, and pH differed for *Microcystis* at exponential and decline phases.
- Interaction between PAC and CPAM dosages was significant during coagulation.
- Fitted models could well predict the actual removal ratio of *Microcystis* by coagulation.
- The removal ratio of *Microcystis* reached 82.49–94.38% with optimized dosages of PAC and CPAM.

This is an Open Access article distributed under the terms of the Creative Commons Attribution Licence (CC BY-NC-ND 4.0), which permits copying and redistribution for non-commercial purposes with no derivatives, provided the original work is properly cited (<http://creativecommons.org/licenses/by-nc-nd/4.0/>).

doi: 10.2166/aqua.2021.110

Weijun Song  
Yu Xie  
Jiapeng Hu  
Xunfang Wu  
College of Ecology and Resources Engineering,  
Wuyi University,  
Wuyishan 354300,  
China

Xi Li  (corresponding author)  
Key Lab of Urban Environment and Health,  
Institute of Urban Environment, Chinese Academy  
of Sciences,  
Xiamen 361021,  
China  
and  
University of Chinese Academy of Sciences,  
Beijing 100049,  
China  
E-mail: [xili@iue.ac.cn](mailto:xili@iue.ac.cn)

## INTRODUCTION

Cyanobacterial bloom has become one of the major environmental problems in lakes and reservoirs worldwide (Liu & Yang 2012; O'Neil *et al.* 2012). In recent years, many countries

have reported that the occurrence of cyanobacterial blooms in resource waters posed a problem for the safety of drinking water. For example, a severe *Microcystis* bloom broke out in Taihu Lake (China) in 2007, resulting in a water crisis for 2 million residents (Zhang et al. 2010). In 2014, toxic cyanobacterial bloom also occurred in Erie Lake (America), and more than 60 people became sick after swallowing the polluted drinking water (Wolf et al. 2017).

In drinking water treatment plants, coagulation is a common treatment to remove cyanobacterial cells in resource waters. Iron salts (e.g., ferric sulfate) or aluminum salts (e.g., aluminum sulfate) are often used as common coagulants to remove cyanobacterial cells (Gonzalez-Torres et al. 2014). In comparison with these common inorganic flocculants, polyaluminum chloride (PAC) is an inorganic polymer flocculant with a large molecular weight, and thus, it has a better flocculating performance attributed to its strong capacity of adsorption and interparticle bridging. Besides, cationic polyacrylamide (CPAM) is an organic macromolecular polymer to aid the coagulation process even with a low dosage, but its high cost always limits application. In recent years, combining PAC and CPAM has been employed in sludge dewatering (Ma et al. 2013; Wang et al. 2019; Wu et al. 2019), microplastics (Zhou et al. 2020), landfill leachate (Shen et al. 2014), slightly polluted source waters (Zhou et al. 2012; Hu et al. 2014), pickle wastewater treatment (Yang et al. 2017), and flue-gas desulfurization wastewater (Zhao 2019). However, there are few reports on cyanobacterial removal by combining PAC and CPAM to improve cyanobacterial removal by coagulation.

When a successive cyanobacterial bloom broke out in resource waters, pH would rise and it even reached 9–10 during cell growth (Visser et al. 2016). Compared with cyanobacteria at the exponential phase, cell viability would strikingly decline, and cellular structures (e.g., gas vesicles and photosynthetic apparatus) were destroyed at the decline phase (Li et al. 2020). Besides, the concentration of extracellular organic matter (EOM) became increased, and its composition was also changed (Henderson et al. 2008; Leloup et al. 2013; Pivokonsky et al. 2014; Li et al. 2020). These changed factors may affect cyanobacterial removal by coagulation. Consequently, in this study, cyanobacteria at exponential and decline phases were prepared for

coagulation experiments. Effects of CPAM dosage, PAC dosage, and pH value on cyanobacterial removal were investigated by measuring chlorophyll *a*. Additionally, a quadratic polynomial mathematical model was established by the response surface design method, aiming to provide a detailed guideline of combining PAC and CPAM to treat cyanobacteria-laden waters.

## MATERIALS AND METHODS

### Cyanobacterial culture

*Microcystis aeruginosa* FACHB-915 was purchased from the Institute of Hydrobiology, Chinese Academy of Sciences. It was cultured in BG11 medium at 28 °C under constant light flux (35  $\mu\text{mol}/\text{m}\cdot\text{s}$ ) with a 12:12 h light–dark cycle in an incubation cabinet equipped with a cold light source, light-emitting diode (GXZ-280C; China), as described in Li et al. (2020). *Microcystis* cells at exponential and decline phases were prepared for coagulation experiments. Prior to coagulation, cyanobacterial solutions were carried out with a dilution of 1:3, and associated water quality parameters are shown in Table 1.

### Reagents and instruments

PAC ( $\text{Al}_2\text{O}_3 > 28\%$ , Sinopharm reagent) was prepared as a stock solution with a concentration of 5.0 g/L, and it was diluted to a 500 mg/L solution for coagulation experiments. CPAM (molecular weight of 12 million, ion degree of 15%) was purchased from a company (Tianjin Dingshengxin Chemical Co. Ltd) and prepared as a stock solution with a

**Table 1** | Water quality parameters of *Microcystis* solutions

| Parameters  | Exponential phase                     | Decline phase                         |
|---|---------------------------------------|---------------------------------------|
| Culture time (days)                                     | 25–30                                 | 65–70                                 |
| Cell density (cells/L)                                  | $0.9 \times 10^6$ – $1.5 \times 10^6$ | $2.9 \times 10^6$ – $3.5 \times 10^6$ |
| pH  | $8.2 \pm 0.2$                         | $9.2 \pm 0.2$                         |
| Chlorophyll <i>a</i> content ( $\mu\text{g}/\text{L}$ ) | $45.0 \pm 2.0$                        | $74.0 \pm 3.0$                        |
| Phycocyanin ( $\mu\text{g}/\text{L}$ )                  | $2,100 \pm 100$                       | $3,800 \pm 150$                       |
| Turbidity (NTU)   | $110 \pm 2.0$                         | $170 \pm 5.0$                         |

concentration of 2.50 g/L. Then, it was diluted to 500 mg/L for coagulation experiments. Additionally, a flow cytometry (FACS Verse, USA), ultrapure water (Millipore Pty Ltd, USA), a fluorometer (FluoroQuik, USA), and a desktop pH meter (UTO, China) were also employed for experiments.

## Experimental protocols

A cyanobacterial solution of 50 mL was transferred into a 100 mL conical flask, and its pH value was adjusted to 6.2–10.2 using 0.1 mol/L NaOH and 0.1 mol/L HCl. Coagulation experiments were carried out with magnetic stirring at the same temperature of  $22 \pm 2$  °C. Various dosages of PAC (2.0–40.0 mol/L) were added to the cyanobacterial solution with rapid mixing at specific intervals. Then, CPAM (1.2–20 mol/L) was added, and these solutions were stirred continuously during the coagulation process (250 rpm/min, 1 min; 150 rpm/min, 4 min; 50 rpm/min, 15 min) with six magnetic agitators and kept motionless for 40 min. Finally, *Microcystis* samples were taken for the measurements of chlorophyll *a*. A total of 17 treatment matrices were conducted based on single-factor experiments and selected three influencing factors such as CPAM dosage, PAC dosage, and pH value. High and low levels were determined by the response value, and then these experiments were performed using the Box–Behnken design (BBD) form (Tables 2 and 3). Finally, response surface methodology (RSM) was employed to analyze these experimental data.

## Analytical methods

Chlorophyll *a* concentration was measured by a two-channel fluorometer (AmiScience, USA). The removal ratio of

chlorophyll *a* was estimated by the following equation.

$$\text{RE}\% = 100 \times (Z1 - Z2)/Z1 \quad (1)$$

where RE% is the removal ratio of chlorophyll *a* via coagulation; Z1 is the chlorophyll *a* concentration before coagulation and Z2 is the chlorophyll *a* concentration after coagulation.

RSM has been widely used to establish a continuous variable surface model, aiming to evaluate these factors that may affect the coagulation process and interactions of these factors, and to determine the best level scope. RSM only required few experimental tests, and thus, it could save manpower and material resources (Li et al. 2015). In this study, this method was employed to optimize the application of combining PAC and CPAM to remove cyanobacteria by the coagulation process.

## Statistics analysis

Three parallel experiments were conducted, and these data were analyzed using Excel 2017. Meanwhile, all data were statistically analyzed using Student's *t*-test, and a significant difference was defined at  $P < 0.05$ . The figures and tables were analyzed with Origin 2017 and Design-Expert 11.

## RESULTS AND DISCUSSION

### Single-factor experiments

#### Effect of CPAM on *Microcystis* removal by coagulation

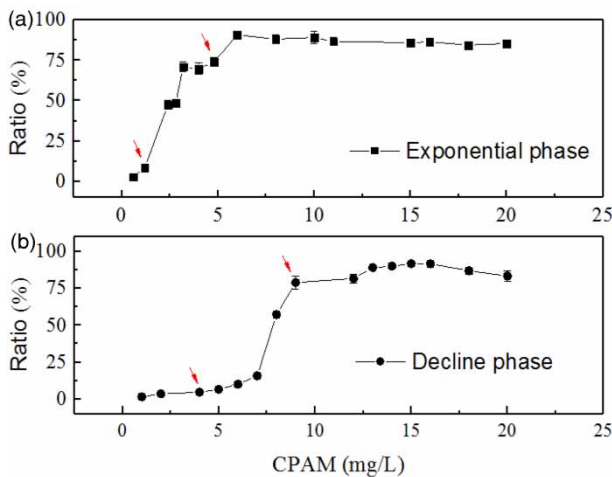
Figure 1 shows that *Microcystis* at the exponential phase is easier to remove than that at the decline phase after dosing

**Table 2** | Variables and levels for BBD experimental design

| Encoding | Factors     | Exponential phase |     |     | Decline phase |      |      |      |
|----------|-------------|-------------------|-----|-----|---------------|------|------|------|
|          |             | Level             |     |     | Level         |      |      |      |
|          |             | - 1               | 0   | 1   |               | - 1  | 0    | 1    |
| A        | CPAM (mg/L) | 1.2               | 3.0 | 4.8 | CPAM (mg/L)   | 4.0  | 6.5  | 9.0  |
| B        | PAC (mg/L)  | 5.0               | 9.0 | 13  | PAC (mg/L)    | 10.0 | 15.0 | 20.0 |
| C        | pH          | 7.2               | 8.2 | 9.2 | pH            | 7.2  | 8.2  | 9.2  |

**Table 3** | BBD experimental design and results

| Removal ratio of chlorophyll <i>a</i> (%) |                   |      |     |                     |               |      |     |                     |
|---|-------------------|------|-----|---------------------|---------------|------|-----|---------------------|
| Serial no.                                | Exponential phase |      |     |                     | Decline phase |      |     |                     |
|   | Level             |      |     | Measurement results | Level         |      |     | Measurement results |
| A   | B                 | C    | A   |                     | B             | C    |     |                     |
| 1   | 1.2               | 5.0  | 8.2 | 28.78               | 4.0           | 10.0 | 8.2 | 31.43               |
| 2   | 4.8               | 5.0  | 8.2 | 54.49               | 9.0           | 10.0 | 8.2 | 38.99               |
| 3   | 1.2               | 13.0 | 8.2 | 35.56               | 4.0           | 20.0 | 8.2 | 83.67               |
| 4   | 4.8               | 13.0 | 8.2 | 75.56               | 9.0           | 20.0 | 8.2 | 92.36               |
| 5   | 1.2               | 9.0  | 7.2 | 38.44               | 4.0           | 15.0 | 7.2 | 49.25               |
| 6   | 4.8               | 9.0  | 7.2 | 42.22               | 9.0           | 15.0 | 7.2 | 47.62               |
| 7   | 1.2               | 9.0  | 9.2 | 16.22               | 4.0           | 15.0 | 9.2 | 46.46               |
| 8   | 4.8               | 9.0  | 9.2 | 56.11               | 9.0           | 15.0 | 9.2 | 67.54               |
| 9   | 3.0               | 5.0  | 7.2 | 53.33               | 6.5           | 10.0 | 7.2 | 29.05               |
| 10  | 3.0               | 13.0 | 7.2 | 46.76               | 6.5           | 20.0 | 7.2 | 89.52               |
| 11  | 3.0               | 5.0  | 9.2 | 27.89               | 6.5           | 10.0 | 9.2 | 46.61               |
| 12  | 3.0               | 13.0 | 9.2 | 52.22               | 6.5           | 20.0 | 9.2 | 87.74               |
| 13  | 3.0               | 9.0  | 8.2 | 78.00               | 6.5           | 15.0 | 8.2 | 82.12               |
| 14  | 3.0               | 9.0  | 8.2 | 79.20               | 6.5           | 15.0 | 8.2 | 81.71               |
| 15  | 3.0               | 9.0  | 8.2 | 85.44               | 6.5           | 15.0 | 8.2 | 83.66               |
| 16  | 3.0               | 9.0  | 8.2 | 78.58               | 6.5           | 15.0 | 8.2 | 82.79               |
| 17  | 3.0               | 9.0  | 8.2 | 78.83               | 6.5           | 15.0 | 8.2 | 82.01               |

**Figure 1** | Effect of CPAM dosage on the removal ratio of chlorophyll *a* for *Microcystis* at exponential and decline phases.

with the same initial dosage of CPAM (Figure 1). When the initial dosage of CPAM increased from 1.2 to 6.0 mg/L, the removal ratio of chlorophyll *a* at the exponential phase

increased from 9.3 to 89.1%, but the removal ratio at the decline phase was only 8.7% (Figure 1). When the initial dosage of CPAM increased to 9.0 mg/L, the removal ratio of chlorophyll *a* significantly increased to 82.1% (Figure 1).

Charge neutralization is one of the mechanisms of cyanobacterial removal at both exponential and decline phases by CPAM coagulation. Previous studies have revealed that cyanobacterial cells at the decline phase exhibited higher zeta potential than those at the exponential phase (Henderson *et al.* 2008; Shi *et al.* 2016). Therefore, cyanobacteria at the decline phase required higher dosages of CPAM to achieve the same removal ratio of cyanobacterial cells.

#### Effect of PAC on *Microcystis* removal by coagulation

Figure 2 shows that *Microcystis* at the exponential phase are still more easily removed than that at the decline phase,

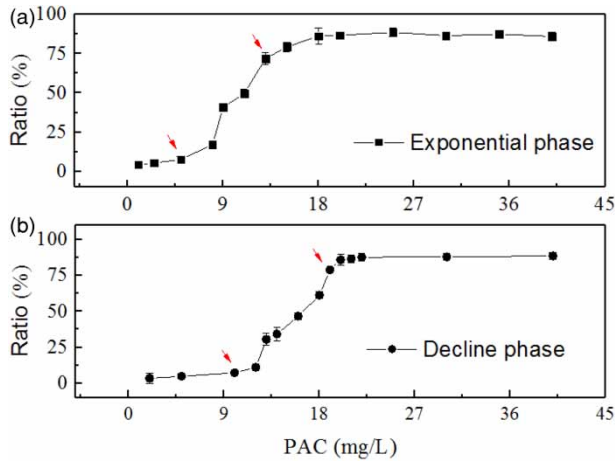


**Figure 2** | Effect of PAC dosage on the removal ratio of chlorophyll *a* for *Microcystis* at exponential and decline phases.

similar to the results of CPAM. Dosing with the initial PAC of 13.0 mg/L, the removal ratio of chlorophyll *a* was about 69.1%. To promote the coagulation efficiency, PAC dosage increased to 18.0 mg/L, and the removal ratio of chlorophyll *a* reached up to 80% (Figure 2). Overall, the removal ratio of chlorophyll *a* was mainly dependent on the dosages of PAC for *Microcystis* at both exponential and decline phases (Figure 2).

Similar to CPAM coagulants, the hydrolysis form of PAC was high-density positively charged substances (Zhang *et al.* 2018; Guo *et al.* 2019). Except for charge neutralization with *Microcystis* cells, the adsorption, bridging,

and netting may further contribute to remove *Microcystis* cells by coagulation. Besides, *Microcystis* cells at the decline phase may release more EOMs and exhibited higher electro-negativity than those at the exponential phase, leading to an increase in PAC consumption.

### Effect of pH on *Microcystis* removal by coagulation

Figure 3 shows that various pH values of 7.2, 8.2, 9.2, and 10.2 are used for coagulation experiments, and CPAM and PAC dosages of 4.0 and 13.0 mg/L are employed to treat *Microcystis* at exponential and decline phases, respectively. At pH values of 7.2–9.2, the removal ratio of chlorophyll *a* at the exponential phase was higher than a pH value of 10.2 after CPAM and PAC coagulation (Figure 3). In contrast, for *Microcystis* at the decline phase, the highest removal ratio of chlorophyll *a* was gained at pH values of 8.2 and 9.2 by CPAM and PAC coagulation, respectively. These results were consistent with previous studies, in that they have noted that pH played an important role in PAC coagulation, since coagulants have different hydrolysis products at various conditions of pH (Duan & Gregory 2003; Hu *et al.* 2006).

### ANOVA of the proposed model

The removal ratio of chlorophyll *a* was used as the response value of the model, and all experimental results are shown

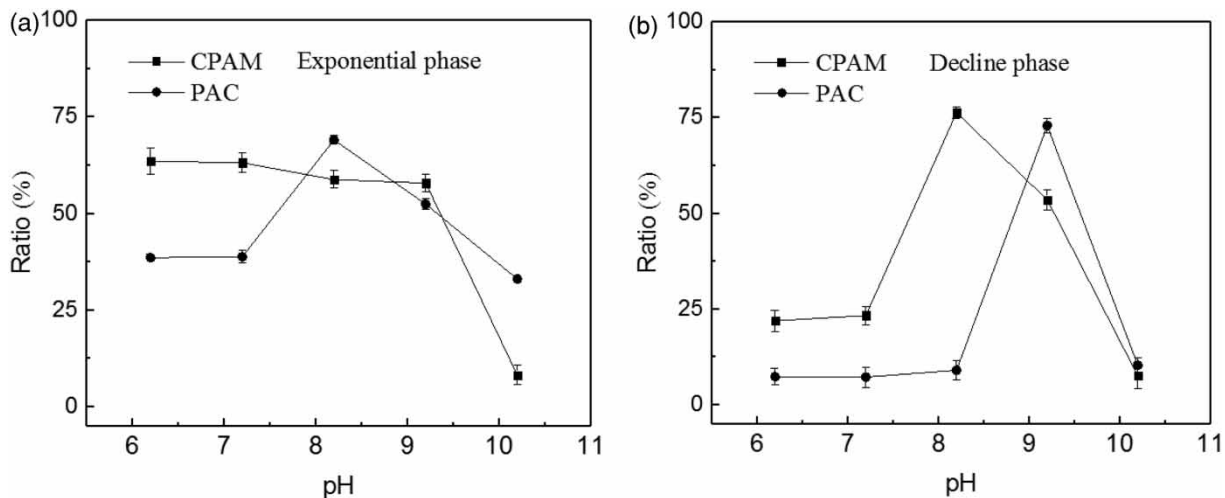


**Figure 3** | Effect of pH on the removal ratio of chlorophyll *a* for *Microcystis* at exponential and decline phases.

in Table 3. The variance analysis of the BBD for the experimental data was conducted using the Design ExpertV11 software, and these results are shown in Table 4. The

**Table 4** | Analysis of variance for the model

| Project      | Exponential phase |          | Decline phase |          |
|--------------|-------------------|----------|---------------|----------|
|              | F-values          | P-values | F-values      | P-values |
| Model        | 44.20             | <0.0001  | 1,056.10      | <0.0001  |
| A            | 81.73             | <0.0001  | 187.89        | <0.0001  |
| B            | 14.21             | 0.0070   | 6,335.6       | <0.0001  |
| C            | 5.48              | 0.0518   | 159.73        | <0.0001  |
| AB           | 2.79              | 0.1388   | 0.38          | 0.5590   |
| AC           | 17.82             | 0.0039   | 152.14        | <0.0001  |
| BC           | 13.06             | 0.0086   | 110.36        | <0.0001  |
| LOF          | 3.20              | 0.1453   | 1.94          | 0.2652   |
| $R^2$        | 0.9827            |          | 0.9993        |          |
| $R^2_{adj}$  | 0.9605            |          | 0.9983        |          |
| $R^2_{pred}$ | 0.7967            |          | 0.9926        |          |
| AP           | 20.727            |          | 90.487        |          |
| CV%          | 7.84              |          | 1.39          |          |

LOF, lack of fit;  $R^2$ , coefficient of determination;  $R^2_{adj}$ , adjusted coefficient of determination;  $R^2_{pred}$ , predicted coefficient of correlation; AP, signal-to-noise ratio; CV, coefficient of variation.

F-values and P-values showed that there were significant correlations between these factors and response values. Table 4 shows that P-values of the two models are below 0.0001, indicating that the fitted model was highly significant and the model could be used for subsequent optimization design. The P-value of misfit (lack of fit) was more than 0.05, suggesting that it was not significant and the model could fit these data well.

The decision coefficients ( $R^2$ ) of the two models were 0.9827 and 0.9993, indicating that there was sufficient consistency between the model prediction and the experimental results (Figure 4). The correction decision coefficients  $R^2_{adj}$  were 0.9605 and 0.9983, demonstrating that the two models can explain the response changes of 96.05 and 99.83% of the data, respectively (Table 4). The difference value of the determination coefficient ( $R^2$ ) and the adjusted determination coefficient  $R^2_{adj}$  were less than 0.2, suggesting that the model held sufficient useful signals, high reliability, and model precision (Table 4). Moreover, it also demonstrated that the model was sufficient to explain the removal ratio of chlorophyll *a* by CPAM, PAC, and pH, and there were no other significant influencing factors to affect the process (Table 4). The signal-to-noise ratio

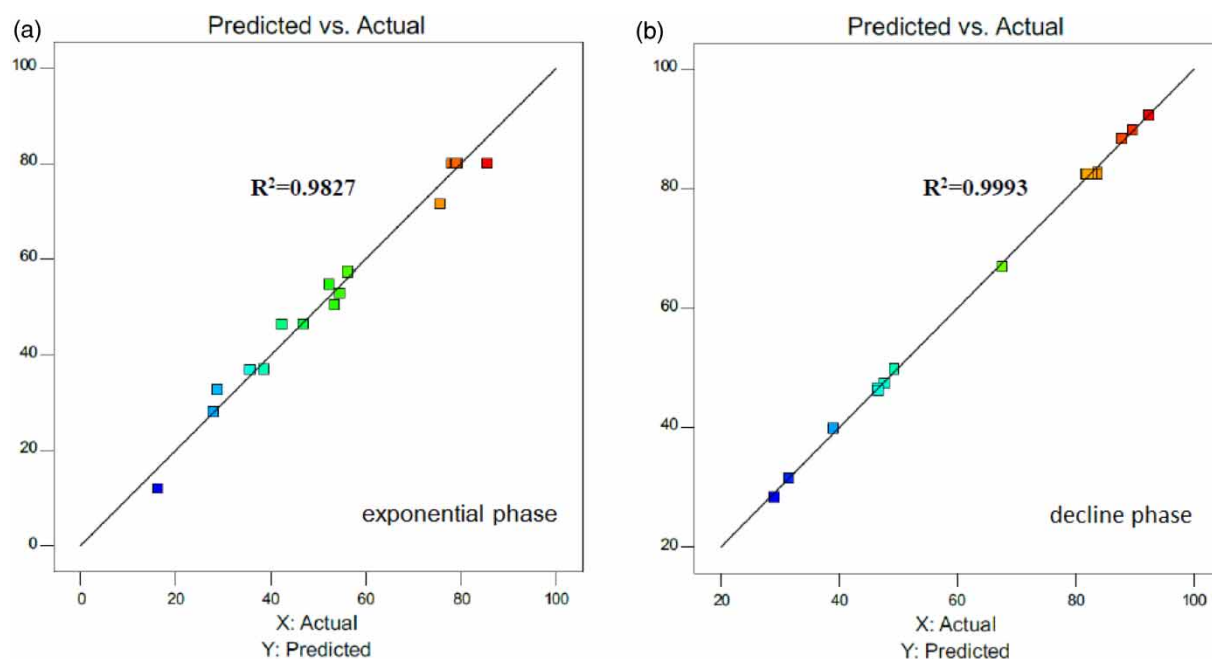


**Figure 4** | A comparison of experimental data vs. predicted data on the removal ratio of chlorophyll *a* based on RSM.

( $AP > 4$ ) further indicated that the fitted models could be used to predict and analyze the removal ratio of chlorophyll *a* under different conditions (Table 4).

Table 4 shows that these values of  $F(A) = 81.73$ ,  $F(B) = 14.21$ , and  $F(C) = 5.48$  are for *Microcystis* at the exponential phase, while  $F(B) = 6,335.6$ ,  $F(A) = 187.89$ , and  $F(C) = 159.73$  are for *Microcystis* at the decline phase. The results suggested that the order of influence on the removal of chlorophyll *a* was different. For *Microcystis* at the exponential phase, the order was CPAM > PAC > pH, and the orders of CPAM > PAC > pH (PAC coagulation) and CPAM > PAC > pH (CPAM coagulation) were for *Microcystis* at the decline phase.

### RSM of the model

RSM analysis could directly reflect these influences and the interaction of these factors (PAC, CPAM, and pH) on the removal ratio of chlorophyll *a*. The projection (contour) of the response surface was a complete ellipse or saddle shape, indicating that the interaction of these factors was significant. In general, the contour arrangement was closer, and the influence of the factors on the removal ratio of chlorophyll was greater.

Figure 5(a)–5(c) show an approximate complete ellipticity for *Microcystis* at the exponential phase.  $P(AC)$  (0.0039) and  $P(BC)$  (0.0086) were less than 0.05, indicating that there was a significant interaction between CPAM and PAC or CPAM and pH. In contrast, Figure 5(d)–5(f) show a completely elliptic for *Microcystis* at the decline phase. The corresponding  $P(AC)$  was below 0.0001 and showed that the interaction between CPAM and PAC was also significant. These results of analysis of variance (ANOVA) and RSM of other factors could not be confirmed, and thus, there was no obvious interaction between these factors.

The comparison analysis of *Microcystis* at exponential and decline phases found that all the PAC axis direction was steeper, and the contour line arrangement was denser. It indicated that the influence of PAC on the removal ratio of chlorophyll *a* for *Microcystis* at the decline phase was greater than that at the exponential phase (Figure 5). Figure 5(e) and 5(f) show that CPAM and PAC carry positive charges to remove *Microcystis* via electrical neutralization. However, pH values of water affecting the

*Microcystis* removal at the decline phase were greater than CPAM, indicating that its mechanism of coagulation was quite different.

During cyanobacterial growth, EOMs would be one of the main factors to affect coagulation (Takaara et al. 2010; Vandamme et al. 2012; Garzon-Sanabria et al. 2013). The cell density of cyanobacterial cells at the exponential phase was low (Pivokonsky et al. 2014; Li et al. 2020), and its positive external charge was lower than the decline phase. Hence, the required dosages of CPAM and PAC were lower for *Microcystis* at the exponential phase than that at the decline phase by coagulation. Besides, at the decline phase, cyanobacterial cells would release EOMs. The EOMs contained amounts of polysaccharides at  $pH > 7.5$ . Among these EOMs,  $\beta$ -hydroxyl acid and  $\gamma$ -hydroxyl acid ( $\beta$ - and  $\gamma$ -COOH) could be fully dissociated, resulting in a large amount of negative charge in the solution aggregation (Safarikova et al. 2013). Consequently, the EOMs held a low zeta potential (Qu et al. 2012). Meanwhile, the negatively charged lipopolysaccharides (LPS) were also produced by cyanobacteria at the decline phase (Garzon-Sanabria et al. 2013). During coagulation, polynucleated Al-hydroxyl polymers were produced by the hydrolysis of PAC  $[Al]_7(OH)_{17}]^{4+}$   $[Al]_{13}(OH)_{34}]^{5+}$  direct action (Duan & Gregory 2003), and it is first neutralized by the negatively charged LPS in the EOMs. It could well explain the increased consumption of CPAM and PAC for the removal of *Microcystis* at the decline stage by coagulation.

PAC plays a major role in coagulation with two hydrolysis products. One is the oligomeric substances of  $Al(OH)_2^{2+}$ ,  $Al(OH)_3^+$ , and  $Al(OH)_3$ , and the other is the polymeric matter of  $Al_7$ ,  $Al_{13}$ , and  $Al_{30}$  (Duan & Gregory 2003). Among these hydrolysis products, polynuclear Al-polymers are the main components in the flocculation process, since they had high charge density. During the coagulation process, the negatively charged EOMs and cyanobacterial cells could be neutralized rapidly, and cyanobacterial cells are easily adsorbed when the zeta potential became zero. CPAM is a long-chain organic polymer, and it has  $COO^-$ ,  $-CONH_2$ ,  $-NH-$ , and other active groups that can collect small colloids to form large particles (Zheng et al. 2016). These positive groups are likely to capture negatively charged cyanobacterial cells and form adsorption bridges,

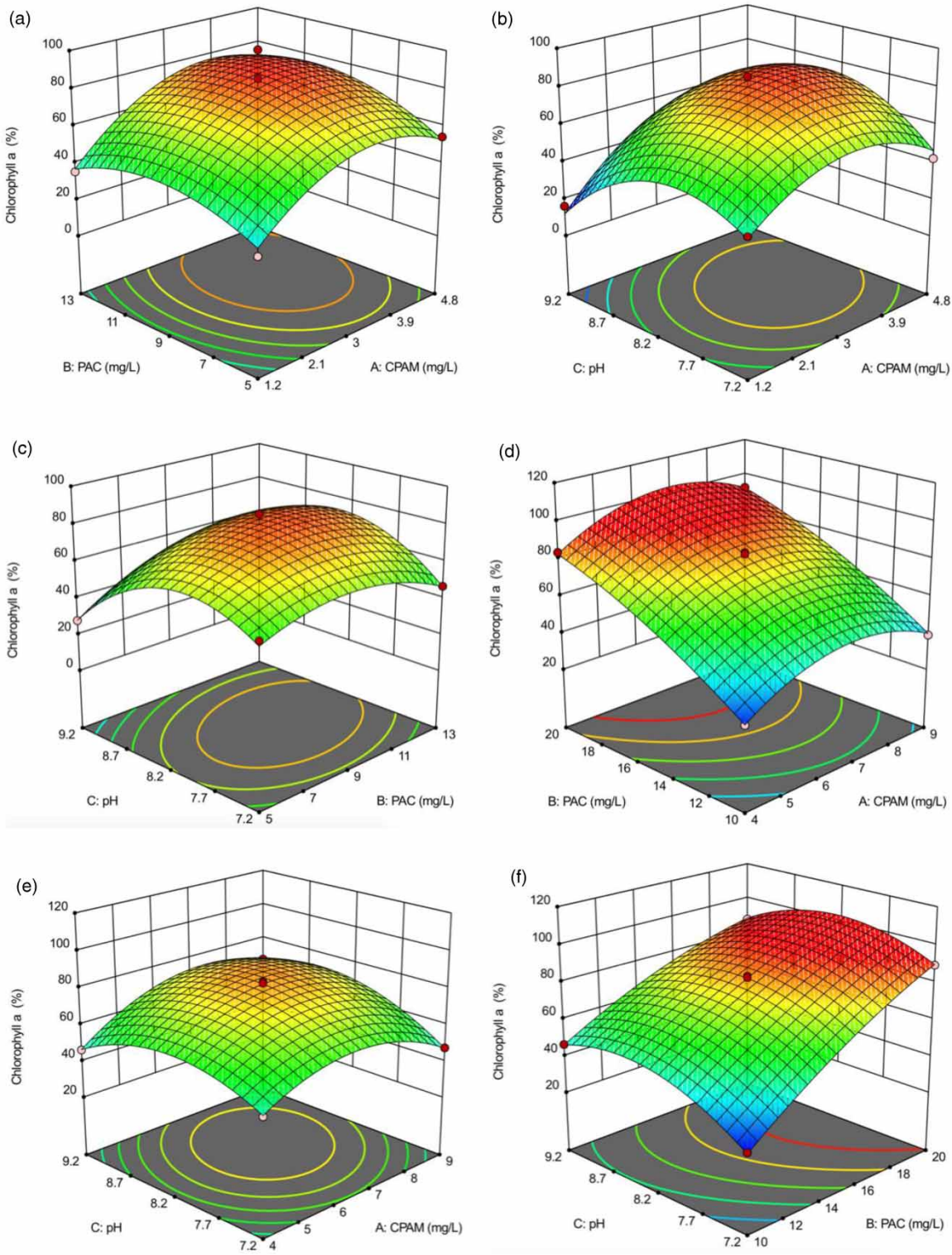


**Figure 5** | Response surface of chlorophyll a removal ratio for exponential and decline phases: (a–c) show the exponential response surface diagram; (d–f) show the decline response surface diagram.



**Table 5** | Predicted values of models and experimental values at optimum conditions

|                   | Regression equation   | CPAM (mg/L) | PAC (mg/L) | pH   | Forecast (%) | Measured values (%) | Relative deviation (%) |
|-------------------|---|-------------|------------|------|--------------|---------------------|------------------------|
| Exponential phase | Chlorophyll <i>a</i> removal ratio (%) = 80.01 + 13.67A + 5.7B – 3.54C + 3.57AB + 9.03AC + 7.73BC – 19.11A <sup>2</sup> – 12.31B <sup>2</sup> – 22.65C <sup>2</sup> | 3.72        | 10.23      | 8.25 | 83.52        | 82.49               | 1.25                   |
|                   |   | 4.77        | 10.21      | 8.17 | 76.47        | 74.96               | 2.01                   |
| Decline phase     | Chlorophyll <i>a</i> removal ratio (%) = 82.46 + 4.46A + 25.9B + 4.11C + 0.282AB + 5.68AC – 4.84BC – 15.68A <sup>2</sup> – 5.17B <sup>2</sup> – 14.06C <sup>2</sup> | 5.98        | 17.81      | 8.21 | 93.75        | 94.38               | 0.67                   |
|                   |   | 6.66        | 18.19      | 8.83 | 92.51        | 90.83               | 1.85                   |

but a competitive flocculation occurs between two cyanobacterial cells in the presence of PAC. The coexistence of PAC resulted in the inhibition of coagulation by mutual restriction between long CPAM chains, and its excess is not conducive to the expansion of the polymer chain structure (Ma et al. 2013; Yu et al. 2019). These characteristics may well explain that the effect of PAC on cyanobacterial removal was greater than CPAM (Figure 5(e) and 5(f)).

### Model validation

RSM showed that the maximum removal ratio of chlorophyll *a* had a better range of process parameters. Using the optimization function of the Design-Expert 11 software, the quadratic regression equation was first-order, and the parameter combination of the maximum removal ratio of chlorophyll *a* under constraint conditions could be obtained. Considering the high pH value of cyanobacteria-laden waters, pH values (8.0–9.0) were selected from the optimized process for the practical verification tests. These measured values were compared with the predicted values of the model, as shown in Table 5. Table 5 shows that the relative deviation between the predicted values of the model and experimental values is 2.01%, demonstrating that the two models could well reflect the effects of the three factors on the removal ratio of chlorophyll *a* for *Microcystis* cells at both exponential and decline phases.

When a cyanobacterial bloom has an outbreak, the pH value of resource waters will be 8.0–9.0. Combining with the model verification in Table 5, the dosages of CPAM and PAC for *Microcystis* at the exponential phase are 3.72 and 10.23 mg/L, respectively, and the removal ratio of *Microcystis* cells could reach up to 83.52%. In this treatment, the relative deviation of the model fitting was low,

and medicament was small. Therefore, this treatment was recommended to treat *Microcystis* at the exponential phase. To achieve the same removal ratio of *Microcystis* at the decline phase, the dosages of CPAM and PAC increased to 5.98 and 17.81 mg/L, respectively, and these dosages were recommended to treat *Microcystis* at the decline phase (Table 5).

### CONCLUSIONS

This study demonstrated that factors of CPAM dosage, PAC dosage, and pH value could strongly affect the removal ratio of *Microcystis* at both exponential and decline phases. Furthermore, the growth phase of cyanobacteria was a key role in the order of influence factors during the coagulation process by combining PAC and CPAM. To achieve the same removal ratio of *Microcystis*, dosages of CPAM and PAC should be higher at the decline phase than that at the exponential phase. Consequently, dosages of CPAM (3.72 mg/L) and PAC (10.23 mg/L) were recommended to treat *Microcystis* at the exponential phase with a pH value of 8.25, and dosages of CPAM and PAC were 5.98 and 17.81 mg/L for *Microcystis* at the decline phase with a pH value of 8.21. These results would provide important technical parameters for cyanobacterial coagulation at exponential and decline phases by combining PAC and CPAM.

### FUNDING

This work was supported by the Fujian Natural Science Foundation Project (no. 2020J01417), the Science and

Technology Project of Water Resources Department of Fujian Province (no. MSK201711), the Science and Technology Major Project of Xiamen (no. 3502Z201710), the National Training Program of Innovation and Entrepreneurship for Undergraduates (no. 201910397006), and the Fujian University Student Innovation Training Project (no. S202010397033).

## DATA AVAILABILITY STATEMENT

Data cannot be made publicly available; readers should contact the corresponding author for details.

## REFERENCES

- Duan, J. & Gregory, J. 2003 Coagulation by hydrolysing metal salts. *Advances in Colloid and Interface Science* **100–102**, 475–502.
- Garzon-Sanabria, A. J., Ramirez-Caballero, S. S., Moss, F. E. P. & Nikolov, Z. L. 2013 Effect of algogenic organic matter (AOM) and sodium chloride on *Nannochloropsis salina* flocculation efficiency. *Bioresource Technology* **143**, 231–237.
- Gonzalez-Torres, A., Putnam, J., Jefferson, B., Stuetz, R. M. & Henderson, R. K. 2014 Examination of the physical properties of *Microcystis aeruginosa* flocs produced on coagulation with metal salts. *Water Research* **60**, 197–209.
- Guo, J. Y., Wen, X. Y., Jia, X. J., Guo, Z. H. & Xu, J. J. 2019 Preparation of magnetic chitosan and improvement of dewatering performance of sludge. *China Environmental Science* **39** (7), 2944–2952.
- Henderson, R. K., Baker, A., Parsons, S. A. & Bruce, J. 2008 Characterisation of algogenic organic matter extracted from cyanobacteria, green algae and diatoms. *Water Research* **42** (13), 3435–3445.
- Hu, C., Liu, H., Qu, J. & Rut, J. 2006 Coagulation behavior of aluminum salts in eutrophic water: significance of Al<sub>13</sub> species and pH control. *Environmental Science & Technology* **40** (1), 325–331.
- Hu, W. C., Wu, C. D., Jia, A. Y. & Liang, W. L. 2014 Enhanced coagulation for treating slightly polluted algae-containing surface water combining polyaluminum chloride (PAC) with diatomite. *Desalination and Water Treatment* **56** (6), 1698–1703.
- Leloup, M., Nicolau, R., Pallier, V., Yéprémian, C. & Feuillade-Cathalifaud, G. 2013 Organic matter produced by algae and cyanobacteria: quantitative and qualitative characterization. *Journal of Environmental Sciences* **25** (6), 1089–1097.
- Li, L., Zhang, S., He, Q. & Hu, X. B. 2015 Application of response surface methodology in experiment design and optimization. *Research and Exploration in Laboratory* **34** (8), 41–45.
- Li, X., Chen, S., Zeng, J., Song, W. & Yu, X. 2020 Comparing the effects of chlorination on membrane integrity and toxin fate of high- and low-viability cyanobacteria. *Water Research* **177**, 115769.
- Liu, J. G. & Yang, W. 2012 Water sustainability for China and beyond. *Science* **337** (6095), 649–650.
- Ma, J. W., Liu, J. W., Cao, R. & Yue, J. B. 2013 Sludge dewaterability with combined conditioning using Fenton's reagent and CPAM. *Environmental Science* **34** (9), 3538–3543.
- Ministry of Environmental Protection of the People's Republic of China (MEPPRC) 2017 *Water Quality – Determination of Chlorophyll a-Spectrophotometric Method*. HJ 897-2017.
- O'Neil, J. M., Davis, T. W., Burford, M. A. & Gobler, C. J. 2012 The rise of harmful cyanobacteria blooms: the potential roles of eutrophication and climate change. *Harmful Algae* **14**, 313–334.
- Pivokonsky, M., Safarikova, J., Baresova, M., Pivokonska, L. & Kopecka, I. 2014 A comparison of the character of algal extracellular versus cellular organic matter produced by cyanobacterium, diatom and green alga. *Water Research* **51**, 37–46.
- Qu, F., Liang, H., Wang, Z., Wang, H., Yu, H. & Li, G. 2012 Ultrafiltration membrane fouling by extracellular organic matters (EOM) of *Microcystis aeruginosa* in stationary phase: Influences of interfacial characteristics of foulants and fouling mechanisms. *Water Research* **46** (5), 1490–1500.
- Safarikova, J., Baresova, M., Pivokonsky, M. & Kopecka, I. 2013 Influence of peptides and proteins produced by cyanobacterium *Microcystis aeruginosa* on the coagulation of turbid waters. *Separation and Purification Technology* **118**, 49–57.
- Shen, L. F., Sun, B. S. & Zhang, Y. 2014 Research on the pretreatment of landfill leachate using composite coagulant of polyaluminium chloride and polyacrylamide. *Industrial Water Treatment* **34** (2), 59–61.
- Shi, W., Tan, W., Wang, L. & Pan, G. 2016 Removal of *Microcystis aeruginosa* using cationic starch modified soils. *Water Research* **97**, 19–25.
- Takaara, T., Sano, D., Masago, Y. & Omura, T. 2010 Surface-retained organic matter of *Microcystis aeruginosa* inhibiting coagulation with polyaluminium chloride in drinking water treatment. *Water Research* **44** (13), 3781–3786.
- Vandamme, D., Foubert, I., Fraeye, I. & Muylaert, K. 2012 Influence of organic matter generated by *Chlorella vulgaris* on five different modes of flocculation. *Bioresource Technology* **124**, 508–511.
- Visser, P. M., Verspagen, J. M. H., Sandrini, G., Stal, L. J., Matthijs, H. C. P., Davis, T. W., Paerl, H. W. & Huisman, J. 2016 How rising CO<sub>2</sub> and global warming may stimulate harmful cyanobacterial blooms. *Harmful Algae* **54**, 145–159.

- Wang, H. F., Hu, H., Wang, H. J. & Zeng, R. J. 2019 Combined use of inorganic coagulants and cationic polyacrylamide for enhancing dewaterability of sewage sludge. *Journal of Cleaner Production* **211**, 387–395.
- Wolf, D., Georgic, W. & Klaiber, H. A. 2017 Reeling in the damages: harmful algal blooms' impact on Lake Erie's recreational fishing industry. *Journal of Environmental Management* **199**, 148–157.
- Wu, W., Zhou, Z., Chen, L., Chen, G. & Wu, Z. 2019 Conditioning for excess sludge and ozonized sludge by ferric salt and polyacrylamide: orthogonal optimization, rheological characteristics and floc properties. *Chemical Engineering Journal* **373**, 1081–1090.
- Yang, H. M., Gu, J. H., Zhang, D. H., Ouyang, J. & Ran, M. 2017 Analysis of flocculant PAC and PAM in the treatment of pickled cabbage wastewater. *Journal of Civil, Architectural & Environmental Engineering* **39** (04), 95–101.
- Yu, W., Wen, Q., Yang, J., Xiao, K., Zhu, Y., Tao, S., Lv, Y., Liang, S., Fan, W., Zhu, S., Liu, Bi., Hou, H. & Hu, J. 2019 Unraveling oxidation behaviors for intracellular and extracellular from different oxidants (HOCl vs. H<sub>2</sub>O<sub>2</sub>) catalyzed by ferrous iron in waste activated sludge dewatering. *Water Research* **148**, 60–69.
- Zhang, X., Chen, C., Ding, J., Ding, J., Hou, A., Li, Y., Niu, Z., Su, X., Xu, Y. & Laws, E. A. 2010 The 2007 water crisis in Wuxi, China: analysis of the origin. *Journal of Hazardous Materials* **182** (1–3), 130–135.
- Zhang, P., Zhao, D. & Wang, Y. L. 2018 Preparation and structural characterization of polyaluminum magnesium titanium chloride. *Research of Environmental Sciences* **31** (12), 2155–2162.
- Zhao, P. F. 2019 Analysis and optimization of flocculation effect of polyaluminium chloride polyacrylamide. *Journal of Liaoning Shihua University* **39** (2), 37–41.
- Zheng, Y. Y., Jiang, J., Sun, Q. Y. & Liu, C. 2016 Effect of different molecular weight and ionic strength of CPAM on sludge dewaterability. *Acta Scientiae Circumstantiae* **36** (8), 2947–2954.
- Zhou, Z., Yang, Y., Li, X., Gao, W., Liang, H. & Li, G. 2012 Coagulation efficiency and flocs characteristics of recycling sludge during treatment of low temperature and micro-polluted water. *Journal of Environmental Sciences* **24** (6), 1014–1020.
- Zhou, G., Wang, Q., Li, J., Li, Q. & Zhang, J. 2020 Removal of polystyrene and polyethylene microplastics using PAC and FeCl<sub>3</sub> coagulation: performance and mechanism. *Science of the Total Environment* **752**, 141837.

First received 26 August 2020; accepted in revised form 14 February 2021. Available online 18 March 2021